Received: 26 May 2020

DOI: 10.1002/mma.6814

RESEARCH ARTICLE

WILEY

Analysis of the fractional corona virus pandemic via deterministic modeling

Nguyen Huy Tuan[1] | **Vo Viet Tri**[2] | **Dumitru Baleanu**[3,4]

[1]Institute of Research and Development, Duy Tan University, Da Nang, 550000, Vietnam

[2]Division of Applied Mathematics, Thu Dau Mot University, Thu Dau Mot, Vietnam

[3]Department of Mathematics, Cankaya University, Ankara, Turkey

[4]Institute of Space Sciences, Magurele-Bucharest, R 76900, Romania

Correspondence
Dumitru Baleanu, Department of Mathematics, Cankaya University, Ankara, Turkey.
Email: dumitru@cankaya.edu.tr

Communicated by: X. J. Yang

With every passing day, one comes to know that cases of the corona virus disease are increasing. This is an alarming situation in many countries of the globe. So far, the virus has attacked as many as 188 countries of the world and 5 549 131 (27 May 2020) human population is affected with 348 224 deaths. In this regard, public and private health authorities are looking for manpower with modeling skills and possible vaccine. In this research paper, keeping in view the fast transmission dynamics of the virus, we have proposed a new mathematical model of eight mutually distinct compartments with the help of memory-possessing operator of Caputo type. The fractional order parameter ψ of the model has been optimized so that smallest error can be attained while comparing simulations and the real data set which is considered for the country Pakistan. Using Banach fixed point analysis, it has been shown that the model has a unique solution whereas its basic reproduction number $\mathcal{R}_0$ is approximated to be 6.5894. Disease-free steady state is shown to be locally asymptotically stable for $\mathcal{R}_0 < 0$, otherwise unstable. Nelder-Mead optimization algorithm under MATLAB Toolbox with daily real cases of the virus in Pakistan is employed to obtain best fitted values of the parameters for the model's validation. Numerical simulations of the model have come into good agreement with the practical observations wherein social distancing, wearing masks, and staying home have proved to be the most effective measures in order to prevent the virus from further spread.

KEYWORDS

basic reproduction number, Caputo fractional derivative, numerical simulations, real data

MSC CLASSIFICATION

34C05; 92D25

1 | INTRODUCTION

It is well known that COVID-19 pandemic has brought a quagmire across the globe whereby more than four million people have been infected globally, apparently, the mortality-recovery ratio is in a positive proportion.[1,2] Nevertheless, by Polymerase Chain Reaction's sensitivity, the absence or presence of the pandemic infected host in previous time is observable and, in the lack of any curative vaccine, the recovery rate seems to be promising. The challenge to health care professionals, the World Health Organization and the Center for Disease Control in every quarter was whether reinfection could occur after a clinically treated COVID-19 patient.

The subtle nature of the ailment has brought the attention of several scientists and medical practitioners to massively embark on multifarious researches in order to fully counterattack and stop the spread of the ailment. A new research in

previous studies[2-4] focuses on the COVID-19 disease outbreak due to the global pandemic phenomenon originating in mainland China. Ming et al.[3] used the popular susceptible-infectious-recovered (SIR) model to obtain optimum values for the model parameters using statistical approach and thus predicted the number of people infected, susceptible, and removed as compared with time. Recently, Ndaırou et al.[5] have proposed a new mathematical model for the transmission of COVID-19 regarding Wuhan based on the 2016 proposed model in Kim et al.[6] and taking into consideration the existence of super-spreaders in the family of corona virus.[7]

The pervasive COVID-19 and the inefficiency of determined and result-based action is an expansive call for more practical and empirical efforts aimed at updating policy models and guidelines for disease control from social and scientific studies. While the already existed researches are concentrated to the disease-free equilibrium and epidemiology where the reproductive number of the infectious population is at its lowest, still researches on this pandemic are not explored. Thus, in order to critically enunciate the actual characteristics of the situation, an expansive study needs to be continuously carried out until we the human-being overcome this so-called enemy COVID-19.

To this aim, we feel motivated to carry out the rigorous study of this pandemic from fractional variant. This is because, it can be noted that, in the recent past, multifarious scientists have shown that the fractional calculus can more precisely explain natural phenomena than the integer calculus.[8-28] In light of this fact, the noninteger calculus becomes increasingly significant and common in the realistic cases modeling, those with memory effects in particular. We feel inspired to investigate and evaluate the fractional variant of the classical model proposed in Ndaırou et al.[5] on COVID-19 pandemic with an effective fractional operator called Caputo fractional derivative. To the best of our knowledge, this is the first time this fractional derivative has been employed for the analysis and investigation of the underlying model.

2 | FORMULATION OF THE MODEL

Based upon the COVID-19 model proposed in Ndaırou et al.[5] and taking into consideration the Caputo fractional operator of order ψ, we have proposed a new model and called it COVID-19 epidemiological model with eight mutually distinct compartments working under the fractional order operator of Caputo type.The main motivation of utilizing a fractional model is due a better description of memory effect. The total human population N is considered to be constant since most of the travel routes have been closed from couple of months and birth and death ratio is assumed to be equal. In this way, it is very much justified for the total population to be constant. Subdivision of the total population is done in eight compartments as follows: (a) $S(t)$—susceptible individuals; (b) $E(t)$—exposed individuals; (c) $I(t)$—symptomatic and infectious individuals; (d) $P(t)$—super-spreader individuals; (e) $A(t)$—asymptomatic individuals; (f) $H(t)$—hospitalized individuals; (g) $R(t)$—recovered individuals; and (h) $D(t)$—dead individuals. The following structure of the COVID-19 model is suggested with the Caputo operator in action:

$$\begin{cases} {}^{C}\mathbb{D}^{\psi}_{0,t}S(t) &= \frac{1}{\Gamma(1-\psi)}\int_0^t (t-\chi)^{-\psi}S'(\chi)d\chi = -\beta^{\psi}\frac{IS}{N} - r\beta^{\psi}\frac{HS}{N} - \beta_s^{\psi}\frac{SP}{N}, \\ {}^{C}\mathbb{D}^{\psi}_{0,t}E(t) &= \frac{1}{\Gamma(1-\psi)}\int_0^t (t-\chi)^{-\psi}E'(\chi)d\chi = \beta^{\psi}\frac{IS}{N} + r\beta^{\psi}\frac{HS}{N} + \beta_s^{\psi}\frac{SP}{N} - \kappa^{\psi}E, \\ {}^{C}\mathbb{D}^{\psi}_{0,t}I(t) &= \frac{1}{\Gamma(1-\psi)}\int_0^t (t-\chi)^{-\psi}I'(\chi)d\chi = \kappa^{\psi}\sigma_e E - (\gamma_h^{\psi} + \gamma_n^{\psi})I - \delta_i^{\psi}I, \\ {}^{C}\mathbb{D}^{\psi}_{0,t}P(t) &= \frac{1}{\Gamma(1-\psi)}\int_0^t (t-\chi)^{-\psi}P'(\chi)d\chi = \kappa^{\psi}\sigma_s E - (\gamma_h^{\psi} + \gamma_n^{\psi})P - \delta_p^{\psi}P, \\ {}^{C}\mathbb{D}^{\psi}_{0,t}A(t) &= \frac{1}{\Gamma(1-\psi)}\int_0^t (t-\chi)^{-\psi}A'(\chi)d\chi = \kappa^{\psi}(1-\sigma_e-\sigma_s)E, \\ {}^{C}\mathbb{D}^{\psi}_{0,t}H(t) &= \frac{1}{\Gamma(1-\psi)}\int_0^t (t-\chi)^{-\psi}H'(\chi)d\chi = \gamma_h^{\psi}(I+P) - \gamma_p^{\psi}H - \delta_h^{\psi}H, \\ {}^{C}\mathbb{D}^{\psi}_{0,t}R(t) &= \frac{1}{\Gamma(1-\psi)}\int_0^t (t-\chi)^{-\psi}R'(\chi)d\chi = \gamma_n^{\psi}(I+P) + \gamma_p^{\psi}H, \\ {}^{C}\mathbb{D}^{\psi}_{0,t}D(t) &= \frac{1}{\Gamma(1-\psi)}\int_0^t (t-\chi)^{-\psi}D'(\chi)d\chi = \delta_i^{\psi}I + \delta_p^{\psi}P + \delta_h^{\psi}H, \end{cases} \tag{1}$$

with $S(0), E(0), I(0), P(0), A(0), H(0), R(0), D(0) \in \mathbb{R}_0^+$. The variables S, E, I, P, A, H, R, D represent the number of individuals who are susceptible, exposed, infectious, super-spreaders, asymptomatic, hospitalized, recovered, and dead; respectively, at any time t. The total population is denoted by $N(t)$. Moreover, $N(t) = S(t) + E(t) + I(t) + P(t) + A(t) + H(t) + R(t) + D(t)$. By adding all the above eight compartments, one can observe that ${}^{C}\mathbb{D}^{\psi}_{0,t}N(t) = 0$, and this is one of the interesting properties of the Caputo operator that its derivative for a constant vanishes, and this property is very well satisfied in the present analysis. Moreover, From first equation of the proposed model (1), one observes that

$$ {}^{C}\mathbb{D}^{\psi}_{0,t}S(t) \leq 0. \tag{2}$$

This, $S(t)$ is always decreasing. In particular, one obtains $S(t) \leq S_0$.

3 | THEORETICAL ANALYSIS OF THE MODEL

In this section, some important properties of the governing model will be investigated.

3.1 | Existence and uniqueness conditions

We start with the existence as well as the uniqueness of the solution for Caputo operator. Take into account a function, real-valued, and continuous depicted by $\mathcal{B}(\mathcal{J})$ is a Banach space on $\mathcal{J} = [0, b]$ with norm $\|(S, E, I, P, A, H, R, D)\| = \|S\| + \|E\| + \|I\| + \|P\| + \|A\| + \|H\| + \|R\| + \|D\|$, $\|S\| = \sup_{t\in\mathcal{J}} |S(t)|$, $\|E\| = \sup_{t\in\mathcal{J}} |E(t)|$, $\|I\| = \sup_{t\in\mathcal{J}} |I(t)|$, $\|P\| = \sup_{t\in\mathcal{J}} |P(t)|$, $\|A\| = \sup_{t\in\mathcal{J}} |A(t)|$, $\|H\| = \sup_{t\in\mathcal{J}} |H(t)|$, $\|R\| = \sup_{t\in\mathcal{J}} |R(t)|$ and $\|D\| = \sup_{t\in\mathcal{J}} |D(t)|$. Employing the Caputo fractional integral on the governing model leads to

$$\begin{aligned}
S(t) - S(0) &= {}^{C}\mathbb{D}^{\psi}_{0,t} \left\{ -\beta^{\psi} \frac{IS}{N} - r\beta^{\psi} \frac{HS}{N} - \beta_s^{\psi} \frac{PS}{N} \right\}, \\
E(t) - E(0) &= {}^{C}\mathbb{D}^{\psi}_{0,t} \left\{ \beta^{\psi} \frac{IS}{N} + r\beta^{\psi} \frac{HS}{N} + \beta_s^{\psi} \frac{PS}{N} - \kappa^{\psi} E \right\}, \\
I(t) - I(0) &= {}^{C}\mathbb{D}^{\psi}_{0,t} \left\{ \kappa^{\psi} \sigma_e E - (\gamma_h^{\psi} + \gamma_r^{\psi}) I - \delta_i^{\psi} I \right\}, \\
P(t) - P(0) &= {}^{C}\mathbb{D}^{\psi}_{0,t} \left\{ \kappa^{\psi} \sigma_s E - (\gamma_h^{\psi} + \gamma_r^{\psi}) P - \delta_p^{\psi} P \right\}, \\
A(t) - A(0) &= {}^{C}\mathbb{D}^{\psi}_{0,t} \left\{ \kappa^{\psi} (1 - \sigma_e - \sigma_s) E \right\}, \\
H(t) - H(0) &= {}^{C}\mathbb{D}^{\psi}_{0,t} \left\{ \gamma_h^{\psi} (I + P) - \gamma_p^{\psi} H - \delta_h^{\psi} H \right\}, \\
R(t) - R(0) &= {}^{C}\mathbb{D}^{\psi}_{0,t} \left\{ \gamma_h^{\psi} (I + P) + \gamma_p^{\psi} H \right\}, \\
D(t) - D(0) &= {}^{C}\mathbb{D}^{\psi}_{0,t} \left\{ \delta_i^{\psi} I + \delta_p^{\psi} P + \delta_h^{\psi} H \right\}.
\end{aligned} \tag{3}$$

The above expressions refer to:

$$\begin{aligned}
S(t) - S(0) &= W(\psi) \int_0^t (t - \chi)^{-\psi} K_1(\psi, \chi, S(\chi)) d\chi, \\
E(t) - E(0) &= W(\psi) \int_0^t (t - \chi)^{-\psi} K_2(\psi, \chi, E(\chi)) d\chi, \\
I(t) - I(0) &= W(\psi) \int_0^t (t - \chi)^{-\psi} K_3(\psi, \chi, I(\chi)) d\chi, \\
P(t) - P(0) &= W(\psi) \int_0^t (t - \chi)^{-\psi} K_4(\psi, \chi, P(\chi)) d\chi, \\
A(t) - A(0) &= W(\psi) \int_0^t (t - \chi)^{-\psi} K_5(\psi, \chi, A(\chi)) d\chi, \\
H(t) - H(0) &= W(\psi) \int_0^t (t - \chi)^{-\psi} K_6(\psi, \chi, H(\chi)) d\chi, \\
R(t) - R(0) &= W(\psi) \int_0^t (t - \chi)^{-\psi} K_7(\psi, \chi, R(\chi)) d\chi, \\
D(t) - D(0) &= W(\psi) \int_0^t (t - \chi)^{-\psi} K_8(\psi, \chi, D(\chi)) d\chi,
\end{aligned} \tag{4}$$

and the kernels are as comes next

$$\begin{aligned}
K_1(\psi, t, S(t)) &= -\beta^{\psi} \frac{IS}{N} - r\beta^{\psi} \frac{HS}{N} - \beta_s^{\psi} \frac{PS}{N}, \\
K_2(\psi, t, E(t)) &= \beta^{\psi} \frac{IS}{N} + r\beta^{\psi} \frac{HS}{N} + \beta_s^{\psi} \frac{PS}{N} - \kappa^{\psi} E, \\
K_3(\psi, t, I(t)) &= \kappa^{\psi} \sigma_e E - (\gamma_h^{\psi} + \gamma_r^{\psi}) I - \delta_i^{\psi} I, \\
K_4(\psi, t, P(t)) &= \kappa^{\psi} \sigma_s E - (\gamma_h^{\psi} + \gamma_r^{\psi}) P - \delta_p^{\psi} P, \\
K_5(\psi, t, A(t)) &= \kappa^{\psi} (1 - \sigma_e - \sigma_s) E, \\
K_6(\psi, t, H(t)) &= \gamma_h^{\psi} (I + P) - \gamma_p^{\psi} H - \delta_h^{\psi} H, \\
K_7(\psi, t, R(t)) &= \gamma_h^{\psi} (I + P) + \gamma_p^{\psi} H, \\
K_8(\psi, t, D(t)) &= \delta_i^{\psi} I + \delta_p^{\psi} P + \delta_h^{\psi} H.
\end{aligned} \tag{5}$$

Now, $K_i(i=1, \ldots, 8)$ must affirm the Lipschitz condition's validity with $S(t)$, $E(t)$, $I(t)$, $P(t)$, $A(t)$, $H(t)$, $R(t)$, and $D(t)$ having an upper bound. Take a couple of functions say $S(t)$ and $S^*(t)$ into consideration, we can write

$$\begin{aligned} &\|K_1(\psi, t, S(t)) - K_1(\psi, t, S^*(t))\| \\ &= \left\| \frac{1}{N}(-\beta^\psi I - r\beta^\psi H - \beta_s^\psi P)(S(t) - S^*(t)) \right\|. \end{aligned} \tag{6}$$

Now, assuming $\Lambda_1 = \left\| \frac{1}{N}\left(-\beta^\psi I - r\beta^\psi H - \beta_s^\psi P\right) \right\|$, we get

$$\|K_1(\psi, t, S(t)) - K_1(\psi, t, S^*(t))\| \leq \Lambda_1 \|S(t) - S^*(t)\|. \tag{7}$$

Continuing in the same way, one gets

$$\begin{aligned} &\|K_2(\psi, t, E(t)) - K_2(\psi, t, E^*(t))\| \leq \Lambda_2 \|E(t) - E^*(t)\|, \\ &\|K_3(\psi, t, I(t)) - K_3(\psi, t, I^*(t))\| \leq \Lambda_3 \|I(t) - I^*(t)\|, \\ &\|K_4(\psi, t, P(t)) - K_4(\psi, t, P^*(t))\| \leq \Lambda_4 \|P(t) - P^*(t)\|, \\ &\|K_5(\psi, t, A(t)) - K_5(\psi, t, A^*(t))\| \leq \Lambda_5 \|A(t) - A^*(t)\|, \\ &\|K_6(\psi, t, H(t)) - K_6(\psi, t, H^*(t))\| \leq \Lambda_6 \|H(t) - H^*(t)\|, \\ &\|K_7(\psi, t, R(t)) - K_7(\psi, t, R^*(t))\| \leq \Lambda_7 \|R(t) - R^*(t)\|, \\ &\|K_8(\psi, t, D(t)) - K_8(\psi, t, D^*(t))\| \leq \Lambda_8 \|D(t) - D^*(t)\|. \end{aligned} \tag{8}$$

We have now shown the satisfaction of the Lipschitz condition for all the kernels. One can recursively gets the expressions in (4) as

$$\begin{aligned} S_n(t) &= W(\psi) \int_0^t (t-\chi)^{-\psi} K_1(\psi, \chi, S_{n-1}(\chi)) d\chi, \\ E_n(t) &= W(\psi) \int_0^t (t-\chi)^{-\psi} K_2(\psi, \chi, E_{n-1}(\chi)) d\chi, \\ I_n(t) &= W(\psi) \int_0^t (t-\chi)^{-\psi} K_3(\psi, \chi, I_{n-1}(\chi)) d\chi, \\ P_n &= W(\psi) \int_0^t (t-\chi)^{-\psi} K_4(\psi, \chi, P_{n-1}(\chi)) d\chi, \\ A_n(t) &= W(\psi) \int_0^t (t-\chi)^{-\psi} K_5(\psi, \chi, A_{n-1}(\chi)) d\chi, \\ H_n(t) &= W(\psi) \int_0^t (t-\chi)^{-\psi} K_6(\psi, \chi, H_{n-1}(\chi)) d\chi, \\ R_n(t) &= W(\psi) \int_0^t (t-\chi)^{-\psi} K_7(\psi, \chi, R_{n-1}(\chi)) d\chi, \\ D_n(t) &= W(\psi) \int_0^t (t-\chi)^{-\psi} K_8(\psi, \chi, D_{n-1}(\chi)) d\chi, \end{aligned} \tag{9}$$

together with $S_0(t) = S(0)$, $E_0(t) = E(0)$, $I_0(t) = I(0)$, $P_0(t) = P(0)$, $A_0(t) = A(0)$, $H_0(t) = H(0)$, $R_0(t) = R(0)$ and $D_0(t) = D(0)$. And then, we have

$$
\begin{aligned}
\Xi_{S,n}(t) &= S_n(t) - S_{n-1}(t) = W(\psi)\int_0^t (t-\chi)^{-\psi}\left(K_1(\psi,\chi,S_{n-1}(\chi)) - K_1(\psi,\chi,S_{n-2}(\chi))\right)d\chi,\\
\Xi_{E,n}(t) &= E_n(t) - E_{n-1}(t) = W(\psi)\int_0^t (t-\chi)^{-\psi}\left(K_2(\psi,\chi,E_{n-1}(\chi)) - K_2(\psi,\chi,E_{n-2}(\chi))\right)d\chi,\\
\Xi_{I,n}(t) &= I_n(t) - I_{n-1}(t) = W(\psi)\int_0^t (t-\chi)^{-\psi}\left(K_3(\psi,\chi,I_{n-1}(\chi)) - K_3(\psi,\chi,I_{n-2}(\chi))\right)d\chi,\\
\Xi_{P,n}(t) &= P_n(t) - P_{n-1}(t) = W(\psi)\int_0^t (t-\chi)^{-\psi}\left(K_4(\psi,\chi,P_{n-1}(\chi)) - K_4(\psi,\chi,P_{n-2}(\chi))\right)d\chi,\\
\Xi_{A,n}(t) &= A_n(t) - A_{n-1}(t) = W(\psi)\int_0^t (t-\chi)^{-\psi}\left(K_5(\psi,\chi,A_{n-1}(\chi)) - K_5(\psi,\chi,A_{n-2}(\chi))\right)d\chi,\\
\Xi_{H,n}(t) &= H_n(t) - H_{n-1}(t) = W(\psi)\int_0^t (t-\chi)^{-\psi}\left(K_6(\psi,\chi,H_{n-1}(\chi)) - K_6(\psi,\chi,H_{n-2}(\chi))\right)d\chi,\\
\Xi_{R,n}(t) &= R_n(t) - R_{n-1}(t) = W(\psi)\int_0^t (t-\chi)^{-\psi}\left(K_7(\psi,\chi,R_{n-1}(\chi)) - K_7(\psi,\chi,R_{n-2}(\chi))\right)d\chi,\\
\Xi_{D,n}(t) &= D_n(t) - D_{n-1}(t) = W(\psi)\int_0^t (t-\chi)^{-\psi}\left(K_8(\psi,\chi,D_{n-1}(\chi)) - K_8(\psi,\chi,D_{n-2}(\chi))\right)d\chi,
\end{aligned}
\tag{10}
$$

It is crucial to consider $S_n(t) = \sum_{i=0}^{n}\Xi_{S,i}(t)$, $E_n(t) = \sum_{i=0}^{n}\Xi_{E,i}(t)$, $I_n(t) = \sum_{i=0}^{n}\Xi_{I,i}(t)$, $P_n(t) = \sum_{i=0}^{n}\Xi_{P,i}(t)$, $A_n(t) = \sum_{i=0}^{n}\Xi_{A,i}(t)$, $H_n(t) = \sum_{i=0}^{n}\Xi_{H,i}(t)$, $R_n(t) = \sum_{i=0}^{n}\Xi_{R,i}(t)$, $D_n(t) = \sum_{i=0}^{n}\Xi_{D,i}(t)$. In addition, from Equations (7) and (8) and supposing that $\Xi_{S,n-1}(t) = S_{n-1}(t) - S_{n-2}(t)$, $\Xi_{E,n-1}(t) = E_{n-1}(t) - E_{n-2}(t)$, $\Xi_{I,n-1}(t) = I_{n-1}(t) - I_{n-2}(t)$, $\Xi_{P,n-1}(t) = P_{n-1}(t) - P_{n-2}(t)$, $\Xi_{A,n-1}(t) = A_{n-1}(t) - A_{n-2}(t)$, $\Xi_{H,n-1}(t) = H_{n-1}(t) - H_{n-2}(t)$, $\Xi_{R,n-1}(t) = R_{n-1}(t) - R_{n-2}(t)$, $\Xi_{D,n-1}(t) = D_{n-1}(t - D_{n-2}(t)$, we attain

$$
\begin{aligned}
\left\|\Xi_{S,n}(t)\right\| &\le W(\psi)\eta_1\int_0^t (t-\chi)^{-\psi}\left\|\Xi_{S,n-1}(\chi)\right\|d\chi,\\
\left\|\Xi_{E,n}(t)\right\| &\le W(\psi)\eta_2\int_0^t (t-\chi)^{-\psi}\left\|\Xi_{E,n-1}(\chi)\right\|d\chi,\\
\left\|\Xi_{I,n}\right\| &\le W(\psi)\eta_3\int_0^t (t-\chi)^{-\psi}\left\|\Xi_{I,n-1}(\chi)\right\|d\chi,\\
\left\|\Xi_{P,n}(t)\right\| &\le W(\psi)\eta_4\int_0^t (t-\chi)^{-\psi}\left\|\Xi_{P,n-1}(\chi)\right\|d\chi,\\
\left\|\Xi_{A,n}(t)\right\| &\le W(\psi)\eta_5\int_0^t (t-\chi)^{-\psi}\left\|\Xi_{A,n-1}(\chi)\right\|d\chi,\\
\left\|\Xi_{H,n}\right\| &\le W(\psi)\eta_6\int_0^t (t-\chi)^{-\psi}\left\|\Xi_{H,n-1}(\chi)\right\|d\chi,\\
\left\|\Xi_{R,n}(t)\right\| &\le W(\psi)\eta_7\int_0^t (t-\chi)^{-\psi}\left\|\Xi_{R,n-1}(\chi)\right\|d\chi,\\
\left\|\Xi_{D,n}(t)\right\| &\le W(\psi)\eta_8\int_0^t (t-\chi)^{-\psi}\left\|\Xi_{D,n-1}(\chi)\right\|d\chi.
\end{aligned}
\tag{11}
$$

Theorem 3.1. *Assume that*

$$
\frac{W(\psi)}{\psi}b^{\psi}\eta_i < 1,\ i = 1, 2, \ldots, 8. \tag{12}
$$

Then, the governing model has a unique solution for $t \in [0,b]$.

Proof. The boundedness of $S(t), E(t), I(t), P(t), A(t), H(t), R(t)$, and $D(t)$ have been proved. Moreover from Equations (7) and (8), $K_1, K_2, K_3, K_4, K_5, K_6, K_7, K_8$ are Lipchitz. Then, Equation (11) together with a recursive hypothesis gives

$$
\begin{aligned}
\left\|\Xi_{S,n}(t)\right\| &\leq \|S_0(t)\| \left(\frac{W(\psi)}{\psi} b^{\psi} \eta_1\right)^n,\\
\left\|\Xi_{E,n}(t)\right\| &\leq \|E_0(t)\| \left(\frac{W(\psi)}{\psi} b^{\psi} \eta_2\right)^n,\\
\left\|\Xi_{I,n}(t)\right\| &\leq \|I_0(t)\| \left(\frac{W(\psi)}{\psi} b^{\psi} \eta_3\right)^n,\\
\left\|\Xi_{P,n}(t)\right\| &\leq \|P_0(t)\| \left(\frac{W(\psi)}{\psi} b^{\psi} \eta_4\right)^n,\\
\left\|\Xi_{A,n}(t)\right\| &\leq \|A_0(t)\| \left(\frac{W(\psi)}{\psi} b^{\psi} \eta_5\right)^n,\\
\left\|\Xi_{H,n}(t)\right\| &\leq \|H_0(t)\| \left(\frac{W(\psi)}{\psi} b^{\psi} \eta_6\right)^n,\\
\left\|\Xi_{R,n}(t)\right\| &\leq \|R_0(t)\| \left(\frac{W(\psi)}{\psi} b^{\psi} \eta_7\right)^n,\\
\left\|\Xi_{D,n}(t)\right\| &\leq \|D_0(t)\| \left(\frac{W(\psi)}{\psi} b^{\psi} \eta_8\right)^n.
\end{aligned} \tag{13}
$$

Thus, $\left\|\Xi_{S,n}\right\| \to 0$, $\left\|\Xi_{E,n}\right\| \to 0$, $\left\|\Xi_{I,n}\right\| \to 0$, $\left\|\Xi_{P,n}\right\| \to 0$, $\left\|\Xi_{A,n}\right\| \to 0$, $\left\|\Xi_{H,n}\right\| \to 0$, $\left\|\Xi_{R,n}\right\| \to 0$, and $\left\|\Xi_{D,n}\right\| \to 0$ as $n \to \infty$. Moreover, from Equation (13) and imposing the triangle inequality, for any k, we have

$$
\begin{aligned}
\|S_{n+k}(t) - S_n(t)\| &\leq \sum_{j=n+1}^{n+k} q_1^j = \frac{q_1^{n+1} - q_1^{n+k+1}}{1-q_1},\\
\|E_{n+k}(t) - E_n(t)\| &\leq \sum_{j=n+1}^{n+k} q_2^j = \frac{q_2^{n+1} - q_2^{n+k+1}}{1-q_2},\\
\|I_{n+k}(t) - I_n(t)\| &\leq \sum_{j=n+1}^{n+k} q_3^j = \frac{q_3^{n+1} - q_3^{n+k+1}}{1-q_3},\\
\|P_{n+k}(t) - P_n(t)\| &\leq \sum_{j=n+1}^{n+k} q_4^j = \frac{q_4^{n+1} - q_4^{n+k+1}}{1-q_4},\\
\|A_{n+k}(t) - A_n(t)\| &\leq \sum_{j=n+1}^{n+k} q_5^j = \frac{q_5^{n+1} - q_5^{n+k+1}}{1-q_5},\\
\|H_{n+k}(t) - H_n(t)\| &\leq \sum_{j=n+1}^{n+k} q_6^j = \frac{q_6^{n+1} - q_6^{n+k+1}}{1-q_6},\\
\|R_{n+k}(t) - R_n(t)\| &\leq \sum_{j=n+1}^{n+k} q_7^j = \frac{q_7^{n+1} - q_7^{n+k+1}}{1-q_7},\\
\|D_{n+k}(t) - D_n(t)\| &\leq \sum_{j=n+1}^{n+k} q_8^j = \frac{q_8^{n+1} - q_8^{n+k+1}}{1-q_8},
\end{aligned} \tag{14}
$$

By hypothesis, it can be noted that $r_i = \frac{W(\psi)}{\psi} b^{\psi} \eta_i < 1$. So, S_n, E_n, I_n, P_n, A_n, H_n, R_n, D_n are regarded as a Cauchy sequences in $\mathcal{B}(\mathcal{J})$. Thus, the uniformly convergent[29] has been reach. Utilizing the proposition on limit in Equation (9) as $n \to \infty$ implies the unique solution of the governing equation. Hence, the existence of a unique solution is reached (12). □

3.2 | Stability analysis and iterative solutions via Caputo fractional derivative

Let $(\mathcal{B}, ||.||)$ be a Banach space and $\mathcal{Q}^*$ be a self-map of $\mathcal{B}$. Also, let us consider the recursive procedure in the form of the $y_{n+1} = h(\mathcal{Q}^*, y_n)$ and $\mathcal{C}(\mathcal{Q}^*)$ be a fixed point set of non-empty $\mathcal{Q}^*$. Here, the sequence y_n converges to the point of

$q^* \in \mathcal{G}(\mathcal{Q}^*)$. Moreover, we define $||z^*_{n+1} - h(\mathcal{Q}^*, z^*_n)||$ such that $\{z^*_n \subseteq \mathcal{B}\}$. The iterative approach, $y_{n+1} = h(\mathcal{Q}^*, y_n)$, is $\mathcal{Q}^*$-stable if $\lim_{n\to\infty} c_n = 0$, that is, $\lim_{n\to\infty} c^*_n = p^*$. For the sequence z_n to be convergent, it must have an upper limit. If all the conditions mentioned above are met for $y_{n+1} = \mathcal{Q}^*$ where n is considered as Picard's iteration as in Wang et al.,[30] then the iteration is $\mathcal{Q}^*$-stable. So, we can express the theorem below:

Let $(\mathcal{B}, ||.||)$ be a Banach space and $\mathcal{Q}^*$ be a self-map on $\mathcal{B}$, then for all $x, y \in \mathcal{B}$, we have

$$\|\mathcal{Q}^*_x - \mathcal{Q}^*_y\| \leq K\|x - \mathcal{Q}^*_x\| + k\|x - y\|, \tag{15}$$

where $K \geq 0$, $0 \leq k < 1$. Assuming $\mathcal{Q}^*$ is Picard $\mathcal{Q}^*$-stable, the recursive formula can be presented as follows:

$$\begin{aligned}
S_{n+1}(t) &= S_n(t) + \mathcal{L}^{-1}\left\{\frac{1}{s^\psi}\mathcal{L}\left\{-\beta^\psi\frac{IS}{N} - r\beta^\psi\frac{HS}{N} - \beta_s^\psi\frac{PS}{N}\right\}\right\},\\
E_{n+1}(t) &= E_n(t) + \mathcal{L}^{-1}\left\{\frac{1}{s^\psi}\mathcal{L}\left\{\beta^\psi\frac{IS}{N} + r\beta^\psi\frac{HS}{N} + \beta_s^\psi\frac{PS}{N} - \kappa^\psi E\right\}\right\},\\
I_{n+1}(t) &= I_n(t) + \mathcal{L}^{-1}\left\{\frac{1}{s^\psi}\mathcal{L}\left\{\kappa^\psi\sigma_e E - (\gamma_h^\psi + \gamma_r^\psi)I - \delta_i^\psi I\right\}\right\},\\
P_{n+1}(t) &= P_n(t) + \mathcal{L}^{-1}\left\{\frac{1}{s^\psi}\mathcal{L}\left\{\kappa^\psi\sigma_s E - (\gamma_h^\psi + \gamma_r^\psi)P - \delta_p^\psi P\right\}\right\},\\
A_{n+1}(t) &= A_n(t) + \mathcal{L}^{-1}\left\{\frac{1}{s^\psi}\mathcal{L}\left\{\kappa^\psi(1 - \sigma_e - \sigma_s)E\right\}\right\},\\
H_{n+1}(t) &= H_n(t) + \mathcal{L}^{-1}\left\{\frac{1}{s^\psi}\mathcal{L}\left\{\gamma_h^\psi(I + P) - \gamma_p^\psi H - \delta_h^\psi H\right\}\right\},\\
R_{n+1}(t) &= R_n(t) + \mathcal{L}^{-1}\left\{\frac{1}{s^\psi}\mathcal{L}\left\{\gamma_h^\psi(I + P) + \gamma_p^\psi H\right\}\right\},\\
D_{n+1}(t = D_n(t) &+ \mathcal{L}^{-1}\left\{\frac{1}{s^\psi}\mathcal{L}\left\{\delta_i^\psi I + \delta_p^\psi P + \delta_h^\psi H\right\}\right\}.
\end{aligned} \tag{16}$$

Let $\mathcal{F}$ be a self-map, then it is defined by

$$\begin{aligned}
\mathcal{F}[S_n(t)] = S_{n+1}(t) &= S_n(t) + \mathcal{L}^{-1}\left\{\frac{1}{s^\psi}\mathcal{L}\left\{-\beta^\psi\frac{IS}{N} - r\beta^\psi\frac{HS}{N} - \beta_s^\psi\frac{PS}{N}\right\}\right\},\\
\mathcal{F}[E_n(t)] = E_{n+1}(t) &= E_n(t) + \mathcal{L}^{-1}\left\{\frac{1}{s^\psi}\mathcal{L}\left\{\beta^\psi\frac{IS}{N} + r\beta^\psi\frac{HS}{N} + \beta_s^\psi\frac{PS}{N} - \kappa^\psi E\right\}\right\},\\
\mathcal{F}[I_n(t)] = I_{n+1}(t) &= I_n(t) + \mathcal{L}^{-1}\left\{\frac{1}{s^\psi}\mathcal{L}\left\{\kappa^\psi\sigma_e E - (\gamma_h^\psi + \gamma_r^\psi)I - \delta_i^\psi I\right\}\right\},\\
\mathcal{F}[P_n(t)] = P_{n+1}(t) &= P_n(t) + \mathcal{L}^{-1}\left\{\frac{1}{s^\psi}\mathcal{L}\left\{\kappa^\psi\sigma_s E - (\gamma_h^\psi + \gamma_r^\psi)P - \delta_p^\psi P\right\}\right\},\\
\mathcal{F}[A_n(t)] = A_{n+1}(t) &= A_n(t) + \mathcal{L}^{-1}\left\{\frac{1}{s^\psi}\mathcal{L}\left\{\kappa^\psi(1 - \sigma_e - \sigma_s)E\right\}\right\},\\
\mathcal{F}[H_n(t)] = H_{n+1}(t) &= H_n(t) + \mathcal{L}^{-1}\left\{\frac{1}{s^\psi}\mathcal{L}\left\{\gamma_h^\psi(I + P) - \gamma_p^\psi H - \delta_h^\psi H\right\}\right\},\\
\mathcal{F}[R_n(t)] = R_{n+1}(t) &= R_n(t) + \mathcal{L}^{-1}\left\{\frac{1}{s^\psi}\mathcal{L}\left\{\gamma_h^\psi(I + P) + \gamma_p^\psi H\right\}\right\},\\
\mathcal{F}[D_n(t] = D_{n+1}(t &= D_n(t) + \mathcal{L}^{-1}\left\{\frac{1}{s^\psi}\mathcal{L}\left\{\delta_i^\psi I + \delta_p^\psi P + \delta_h^\psi H\right\}\right\}.
\end{aligned} \tag{17}$$

which is $\mathcal{F}$-stable in $L^1(a, b)$ if the following conditions are satisfied

$$\begin{cases}
\left\{1 - \beta^\psi(Q_1 + Q_3)f_1(\rho) - r\beta^\psi(Q_1 + Q_6)f_2(\rho) - \beta_s^\psi(Q_1 + Q_4)f_3(\rho)\right\} < 1,\\
\left\{1 - \beta^\psi(Q_1 + Q_3)f_4(\rho) + r\beta^\psi(Q_1 + Q_6)f_5(\rho) + \beta_s^\psi(Q_1 + Q_4)f_6(\rho) - \kappa^\psi K_1\right\} < 1,\\
\left\{1 - \left(\kappa^\psi\sigma_e - (\gamma_h^\psi + \gamma_r^\psi) - \delta_i^\psi\right)K_2\right\} < 1,\\
\left\{1 - \left(\kappa^\psi\sigma_s - (\gamma_h^\psi + \gamma_r^\psi) - \delta_p^\psi\right)K_3\right\} < 1,\\
\left\{1 - \kappa^\psi\left(1 - \sigma_e - \sigma_s\right)K_4\right\} < 1,\\
\left\{1 - \left(\gamma_h^\psi - \gamma_p^\psi - \delta_h^\psi\right)K_5\right\} < 1,\\
\left\{1 - \left(\gamma_h^\psi + \gamma_p^\psi\right)K_6\right\} < 1,\\
\left\{1 - \left(\delta_i^\psi + \delta_p^\psi + \delta_h^\psi\right)K_7\right\} < 1.
\end{cases} \tag{18}$$

Proof. It is clear that $\mathcal{F}$ is a fixed point. So, we determine the following iterations for all $(m, n) \in \mathbb{N} \times \mathbb{N}$.

$$\begin{aligned}
\mathcal{F}(S_n(t)) - \mathcal{F}(S_m(t)) &= S_n(t) - S_m(t),\\
\mathcal{F}(E_n(t)) - \mathcal{F}(E_m(t)) &= E_n(t) - E_m(t),\\
\mathcal{F}(I_n(t)) - \mathcal{F}(I_m(t)) &= I_n(t) - I_m(t),\\
\mathcal{F}(P_n(t)) - \mathcal{F}(P_m(t)) &= P_n(t) - P_m(t),\\
\mathcal{F}(A_n(t)) - \mathcal{F}(A_m(t)) &= A_n(t) - A_m(t),\\
\mathcal{F}(H_n(t)) - \mathcal{F}(H_m(t)) &= H_n(t) - H_m(t),\\
\mathcal{F}(R_n(t)) - \mathcal{F}(R_m(t)) &= R_n(t) - R_m(t),\\
\mathcal{F}(D_n(t)) - \mathcal{F}(F_m(t)) &= D_n(t) - F_m(t)
\end{aligned} \tag{19}$$

Taking the norm of both sides of the first equation in (19), we have

$$\begin{aligned}
\|\mathcal{F}(S_n(t)) - \mathcal{F}(S_m(t))\| = \|S_n(t) - S_m(t) + \mathcal{L}^{-1}\left\{\frac{1}{s^\psi}\mathcal{L}\left\{-\beta^\psi \frac{I_n S_n}{N} - r\beta^\psi \frac{H_n S_n}{N} - \beta_s^\psi \frac{P_n S_n}{N}\right\}\right\}\\
- \mathcal{L}^{-1}\left\{\frac{1}{s^\psi}\mathcal{L}\left\{-\beta^\psi \frac{I_m S_m}{N} - r\beta^\psi \frac{H_m S_m}{N} - \beta_s^\psi \frac{P_m S_m}{N}\right\}\right\}\|,
\end{aligned} \tag{20}$$

and if we use the triangular inequality, we can write

$$\begin{aligned}
\|\mathcal{F}(S_n(t)) - \mathcal{F}(S_m(t))\| = \|S_n(t) - S_m(t)\| + \|\mathcal{L}^{-1}\left\{\frac{1}{s^\psi}\mathcal{L}\left\{-\beta^\psi \frac{I_n S_n}{N} - r\beta^\psi \frac{H_n S_n}{N} - \beta_s^\psi \frac{P_n S_n}{N}\right\}\right\}\\
- \mathcal{L}^{-1}\left\{\frac{1}{s^\psi}\mathcal{L}\left\{-\beta^\psi \frac{I_m S_m}{N} - r\beta^\psi \frac{H_m S_m}{N} - \beta_s^\psi \frac{P_m S_m}{N}\right\}\right\}\|.
\end{aligned} \tag{21}$$

By some necessary simplifications, (21) takes the form of

$$\begin{aligned}
\|\mathcal{F}(S_n(t)) - \mathcal{F}(S_m(t))\| \le \|S_n(t) - S_m(t)\| + \mathcal{L}^{-1}\left\{\frac{1}{s^\psi}\mathcal{L}\left\{\|\frac{-\beta^\psi S_n}{N}(I_n - I_m)\| + \|\frac{-\beta^\psi I_n}{N}(S_n - S_m)\|\right.\right.\\
\left.\left. + \|\frac{-r\beta^\psi S_n}{N}(H_n - H_m)\| + \|\frac{-r\beta^\psi H_n}{N}(S_n - S_m)\| + \|\frac{-\beta_s^\psi S_n}{N}(P_n - P_m)\| + \|\frac{-\beta_s^\psi P_n}{N}(S_n - S_m)\|\right\}\right\}.
\end{aligned} \tag{22}$$

Owing to the same behavior of functions inside the system handled, it can be assumed that

$$\begin{aligned}
\|H_n(t) - H_m(t)\| &\cong \|S_n(t) - S_m(t)\|\\
\|I_n(t) - I_m(t)\| &\cong \|S_n(t) - S_m(t)\|\\
\|P_n(t) - P_m(t)\| &\cong \|S_n(t) - S_m(t)\|.
\end{aligned} \tag{23}$$

Substituting (23) into the relation (22), we reach

$$\begin{aligned}
\|\mathcal{F}(S_n(t)) - \mathcal{F}(S_m(t))\| \le \|S_n(t) - S_m(t)\| + \mathcal{L}^{-1}\left\{\frac{1}{s^\psi}\mathcal{L}\left\{\|\frac{-\beta^\psi S_n}{N}(S_n - S_m)\| + \|\frac{-\beta^\psi I_n}{N}(S_n - S_m)\|\right.\right.\\
\left.\left. + \|\frac{-r\beta^\psi S_n}{N}(S_n - S_m)\| + \|\frac{-r\beta^\psi H_n}{N}(S_n - S_m)\| + \|\frac{-\beta_s^\psi S_n}{N}(S_n - S_m)\| + \|\frac{-\beta_s^\psi P_n}{N}(S_n - S_m)\|\right\}\right\}.
\end{aligned} \tag{24}$$

Because the sequences $S_n(t)$, $H_m(t)$, $I_m(t)$, and $P_m(t)$ are convergent and bounded, there exist four different constants $S_1 > 0$, $S_2 > 0$, S_3 and $S_4 > 0$ for all t. Hence, we have

$$\|S_n(t)\| < S_1, \|H_m(t)\| < S_2, \|P_m(t)\| < S_3, \|I_m(t)\| < S_4, (m, n) \in \mathbb{N} \times \mathbb{N}. \tag{25}$$

By the relations (24) and (25), one can attain

$$\|\mathcal{F}(S_n(t)) - \mathcal{F}(S_m(t))\| \leq \left[1 - \beta^{\psi}(Q_1+Q_3)f_1(\rho) - r\beta^{\psi}(Q_1+Q_6)f_2(\rho) - \beta_s^{\psi}(Q_1+Q_4)f_3(\rho)\right] \|(S_n(t) - S_m(t))\|, \tag{26}$$

where f_1, g_1, and k_1 are the functions obtained by the inverse Laplace transform in (24). In a similar manner, we reach

$$\begin{aligned}
&\|\mathcal{F}(E_n(t)) - \mathcal{F}(E_m(t))\| \leq [1 - \beta^{\psi}(Q_1+Q_3)f_4(\rho) + r\beta^{\psi}(Q_1+Q_6)f_5(\rho) + \beta_s^{\psi}(Q_1+Q_4)f_6(\rho) - \kappa^{\psi}K_1]\|E_n(t) - E_m(t)\|,\\
&\|\mathcal{F}(I_n(t)) - \mathcal{F}(I_m(t))\| \leq [1 - \left(\kappa^{\psi}\sigma_e - (\gamma_h^{\psi} + \gamma_r^{\psi}) - \delta_i^{\psi}\right) K_2]\|I_n(t) - I_m(t)\|,\\
&\|\mathcal{F}(P_n(t)) - \mathcal{F}(P_m(t))\| \leq [1 - \left(\kappa^{\psi}\sigma_s - (\gamma_h^{\psi} + \gamma_r^{\psi}) - \delta_p^{\psi}\right) K_3]\|P_n(t) - P_m(t)\|,\\
&\|\mathcal{F}(A_n(t)) - \mathcal{F}(A_m(t))\| \leq [1 - \kappa^{\psi}\left(1 - \sigma_e - \sigma_s\right) K_4]\|A_n(t) - A_m(t)\|,\\
&\|\mathcal{F}(H_n(t)) - \mathcal{F}(H_m(t))\| \leq [1 - \left(\gamma_h^{\psi} - \gamma_p^{\psi} - \delta_h^{\psi}\right) K_5]\|H_n(t) - H_m(t)\|,\\
&\|\mathcal{F}(R_n(t)) - \mathcal{F}(R_m(t))\| \leq [1 - \left(\gamma_h^{\psi} + \gamma_p^{\psi}\right) K_6]\|R_n(t) - R_m(t)\|,\\
&\|\mathcal{F}(D_n(t) - \mathcal{F}(D_m(t))\| \leq [1 - \left(\delta_i^{\psi} + \delta_p^{\psi} + \delta_h^{\psi}\right) K_7]\|D_n(t) - D_m(t)\|.
\end{aligned} \tag{27}$$

Hence, the prove is complete. □

3.3 | Basic reproduction number

As a proxy for the spread of disease in a population, the basic reproduction number (BRN) plays a significant role in the course and control of a continuing outbreak. It can be understood as the average number of cases produced by one infected person in an otherwise uninfected population over the course of their infectious time. Employing the next generation matrix to the governing model as stated in Baleanu et al.,[13] the BRN can be determined using the following matrices of generation F and V:

$$F = \begin{pmatrix} 0 & \beta^{\psi} & \beta^{\psi} r & \beta_s^{\psi} \\ 0 & 0 & 0 & 0 \\ 0 & 0 & 0 & 0 \\ 0 & 0 & 0 & 0 \end{pmatrix} \text{and } V = \begin{pmatrix} \kappa^{\psi} & 0 & 0 & 0 \\ -\kappa^{\psi}\sigma_e & \gamma_h^{\psi} + \gamma_r^{\psi} + \delta_i^{\psi} & 0 & 0 \\ -\kappa^{\psi}\sigma_s & 0 & \gamma_h^{\psi} + \gamma_r^{\psi} + \delta_p^{\psi} & 0 \\ 0 & -\gamma_h^{\psi} & -\gamma_h^{\psi} & \gamma_p^{\psi} + \delta_h^{\psi} \end{pmatrix}.$$

Consequently, the BRN is obtained by the following expression:

$$R_0 = \frac{\beta^{\psi}\sigma_e(\gamma_h^{\psi} r + \gamma_p^{\psi} + \delta_h^{\psi})}{(\gamma_h^{\psi} + \gamma_r^{\psi} + \delta_i^{\psi})(\gamma_p^{\psi} + \delta_h^{\psi})} + \frac{(\beta^{\psi}\gamma_h^{\psi} r + \beta_s^{\psi}(\gamma_p^{\psi} + \delta_h^{\psi}))\sigma_s}{(\gamma_h^{\psi} + \gamma_p^{\psi} + \delta_p^{\psi})(\gamma_p^{\psi} + \delta_h^{\psi})}. \tag{28}$$

The above expression of the BRN gives a measuring tools of the ailments risk during the COVID-19 outbreak.

Theorem 3.2. *The disease-free equilibrium (DE) E_0, of the governing model (1), is locally asymptotically stable in the given region when $R_0 < 1$, and unstable when $R_0 > 1$.*

Employing the techniques provided in Van den Driessche and Wanmough,[31] it can be seen that when the BRN is less than one, the DE is stable locally and no disease invasion can be found in the population. The proof of (3.2) follows.

4 | ESTIMATION OF PARAMETERS

Parameter estimation is one of the most important steps to be taken in order to know about values of some nondemographic parameters of the epidemiological models. Without this estimation, it is almost impossible to go with the analysis and validation of the proposed models in the areas of mathematical biology. Some of the parameters in the model can easily be obtained with the help of geographical data available for the country or the region of interest, that is, the region for which actual data of the epidemic under investigation is available. Some such parameters could be the recruitment rate of the population of the region, death rate, birth rate, and recovery rate of the affected ones. In the current study, we have chosen data for Pakistan from (http://covid.gov.pk/stats/pakistan) wherein actual cases of the pandemic are being recorded on daily basis. Based upon the availability of this data set, we have selected cases from 01 April 2020 to 10 May

2020 while preparing this research work. In this way, 40 data points are available in order to simulate the model for the symptomatic and infectious class - $I(t)$. The amount of data is fairly good enough for validation of the proposed COVID-19 model. While looking at the model, one can observe that it does not have any demo-graphical parameter and therefore we need to get each parameter through estimation technique. Now the technique used in the present study is the nonlinear least-squares curve fitting technique which is one of the most frequently used techniques for such purposes as can be found in recent studies.[32,33] Thus, the application of the nonlinear least-squares curve fitting technique via Optimization Toolbox routine of MATLAB called ***fminsearch*** from the Matlab Optimization Toolbox has been carried out. The Nelder-Mead optimization algorithm is the basic element of this routine, and it implements the objective function based on the least square technique. Provided a theoretical model $t \mapsto \Theta(t, a_1, a_2, \ldots, a_m)$, depending on some unknown parameters $a_1, a_2, \ldots, a_m$ and a sequence of data points $(t_0, y_0), \ldots, (t_i, y_i)$, the goal remains to determine values of the parameters such as the error

$$E := \sqrt{\sum_{j=0}^{i} \left(\Theta(t, a_1, a_2, \ldots, a_m) - y_j\right)^2}, \tag{29}$$

achieves a minimum. This is how we obtained best fitted values of unknown parameters of the proposed model in the Caputo sense. It is also worth to be mentioned that the fractional order parameter ψ which is the major concern of the present study has also been optimized. This is one the novel features of our research finding since most of the recent researches do consider epidemiological models in the field of fractional calculus and obtain the best values for biological parameters but they do not determine optimized value for the fractional parameter itself. The best fitted values of the model's parameters in both classical and fraction version are listed in Tables 1 and 2, respectively.

It can be observed in Figures 1 and 2 that the curve of the symptomatic and infectious population $I(t)$ agrees better with the real data for daily cases of the virus in Pakistan from 01 April 2020 to 10 May 2020 under the Caputo version as compared to the classical one whereas residuals have been shown in Figures 3 and 4, respectively. This builds confidence to have more power assigned with the fractional operator of Caputo type. The average absolute relative error is found to be comparatively smaller which is about $1.5098e-02$ in the Caputo case and $7.02746e-02$ in the classical version. Thus, it proves superiority of the Caputo operator over the classical (integer-order) operator.

β	**Transmission rate due to infected individuals**	**1.388282e+00**
β_s	Transmission rate due to super-spreaders	0.0946423916
r	Relative transmissibility of hospitalized individuals	0.0000029347
κ	Rate for exposed to become infectious	1.5926870796
σ_e	Rate of exposed to become symptomatic and infectious	0.0551302408
σ_s	Rate of exposed to become super-spreader	0.0000096901
γ_h	Rate of hospitalization	0.0008155133
γ_n	Recovery rate without being hospitalized	0.0026888377
γ_p	Recovery rate of hospitalized patients	0.1650165379
δ_i	Disease induced death rate due to class I	0.0035502729
δ_p	Disease induced death rate due to super-spreaders	0.0012250334
δ_h	Death rate due to hospitalization for disease	0.0205088559

TABLE 1 Best fitted parameters of the classical ($\psi = 1$) version of COVID-19 model (1)

ψ	**Fractional order**	**$5.245e-01$**
β	Transmission rate due to infected individuals	1.388282e+00
β_s	Transmission rate due to super-spreaders	0.3443080149
r	Relative transmissibility of hospitalized individuals	3.677347e-01
κ	Rate for exposed to become infectious	1.5926870796
σ_e	Rate of exposed to become symptomatic and infectious	0.2741625219
σ_s	Rate of exposed to become super-spreader	0.2761296879
γ_h	Rate of hospitalization	0.0183468690
γ_n	Recovery rate without being hospitalized	0.0072702216
γ_p	Recovery rate of hospitalized patients	0.0002074216
δ_i	Disease induced death rate due to class I	0.0034410900
δ_p	Disease induced death rate due to super-spreaders	0.0308516602
δ_h	Death rate due to hospitalization for disease	0.0001249332

TABLE 2 Best fitted parameters of the proposed COVID-19 model (1)

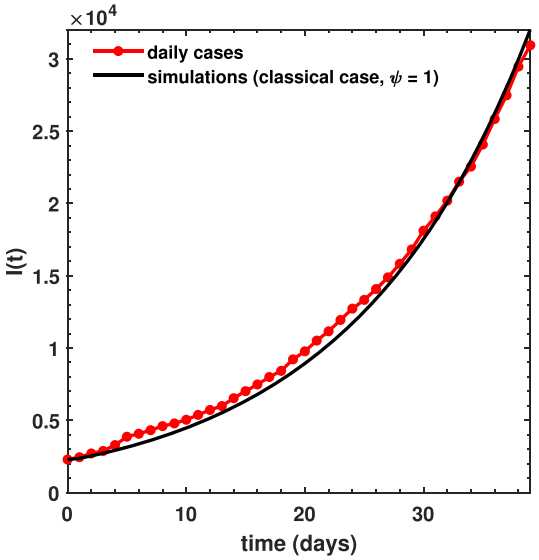

FIGURE 1 Data fitting for the COVID-19 daily cases (solid red line with red circles) in Pakistan from 01 April to 10 May 2020 with the symptomatic and infectious class $I(t)$ (solid black line) of the model under the classical case ($\psi = 1$) [Colour figure can be viewed at wileyonlinelibrary.com]

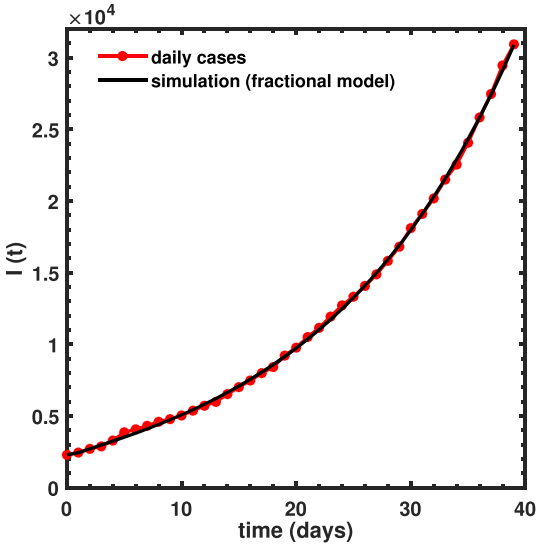

FIGURE 2 Data fitting for the COVID-19 daily cases (red asterisks) in Pakistan from 01 April to 10 May 2020 with the symptomatic and infectious class $I(t)$ (solid black line) of the proposed model under the Caputo operator using optimized value of $\psi = 5.245e-01$ [Colour figure can be viewed at wileyonlinelibrary.com]

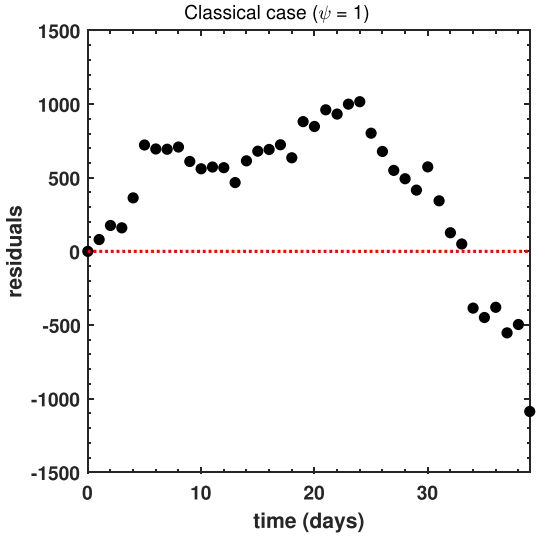

FIGURE 3 Scattering of residuals for the classical COVID-19 model ($\psi = 1$) with daily cases in Pakistan from 01 April to 10 May 2020 [Colour figure can be viewed at wileyonlinelibrary.com]

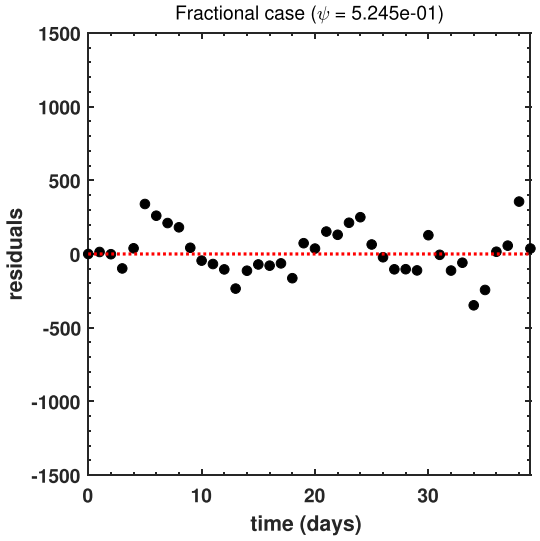

FIGURE 4 Scattering of residuals for the COVID-19 daily cases in Pakistan from 01 April to 10 May 2020 [Colour figure can be viewed at wileyonlinelibrary.com]

5 | NUMERICAL SIMULATIONS: A CASE STUDY OF PAKISTAN

This is where we present various numerical results for the proposed COVID-19 model with the help of best fitted parameters as obtained in the Table 2 while using a fractional differential operator known with the name of Caputo. A predictor-corrector Adams-type scheme for the fractional type of dynamical systems as introduced and analyzed in previous studies[34-36] has been utilized to serve the purpose of simulations of the model. The following structure of the Cauchy ordinary differential equation is taken into consideration in terms of the Caputo differential operator of order ψ:

$$ {}_0^C D_t^{\psi} \varphi(t) = \Phi(t, \varphi(t)), \varphi^{(p)}(0) = \varphi_0^p, 0 < \psi \leq 1, 0 < t \leq \tau, \tag{30} $$

where $p = 0, 1, \ldots, n-1, n = \lceil \psi \rceil$. The Volterra equation version of Equation (30) can be written in the following way:

$$ \varphi(t) = \sum_{p=0}^{n-1} \varphi_0^{(p)} \frac{t^p}{p!} + \frac{1}{\Gamma(\psi)} \int_0^t (t-s)^{\psi-1} \Phi(s, \varphi(s))\, ds. \tag{31} $$

By using the above described predictor-corrector type of scheme related with the Adam-Bashforth-Moulton solver[35] to obtain the approximate solutions of the fractional order COVID-19 model, we have assumed $h = \tau/N$, $t_j = jh$, and $j = 0,1, \ldots, N \in Z^+$, by assuming $\varphi_j \approx \varphi(t_j)$, where φ_j stands for the approximate solution and $\varphi(t_j)$ for the true one. It can now be discretized in the following manner, that is, the corresponding corrector part becomes the following

$$
\begin{aligned}
S_{k+1} &= \sum_{j=0}^{k-1} S_0^{(j)} \frac{t_{k+1}^j}{j!} + \frac{h^{\psi}}{\Gamma(\psi+2)} \sum_{j=0}^{k} (q_{j,k+1}) \left(-\beta^{\psi} \frac{I_j S_j}{N_j} - r\beta^{\psi} \frac{H_j S_j}{N_j} - \beta_s^{\psi} \frac{S_j P_j}{N_j} \right) \\
&\quad + \frac{h^{\psi}}{\Gamma(\psi+2)} \sum_{j=0}^{k} (q_{k+1,k+1}) \left(-\beta^{\psi} \frac{I_{k+1}^p S_{k+1}^p}{N_{k+1}^p} - r\beta^{\psi} \frac{H_{k+1}^p S_{k+1}^p}{N_{k+1}^p} - \beta_s^{\psi} \frac{S_{k+1}^p P_{k+1}^p}{N_{k+1}^p} \right), \\
E_{k+1} &= \sum_{j=0}^{k-1} E_0^{(j)} \frac{t_{k+1}^j}{j!} + \frac{h^{\psi}}{\Gamma(\psi+2)} \sum_{j=0}^{k} (q_{j,k+1}) \left(\beta^{\psi} \frac{I_j S_j}{N_j} + r\beta^{\psi} \frac{H_j S_j}{N_j} + \beta_s^{\psi} \frac{S_j P_j}{N_j} - \kappa^{\psi} E_j \right) \\
&\quad + \frac{h^{\psi}}{\Gamma(\psi+2)} \sum_{j=0}^{k} (q_{k+1,k+1}) \left(\beta^{\psi} \frac{I_{k+1}^p S_{k+1}^p}{N_{k+1}^p} + r\beta^{\psi} \frac{H_{k+1}^p S_{k+1}^p}{N_{k+1}^p} + \beta_s^{\psi} \frac{S_{k+1}^p P_{k+1}^p}{N_{k+1}^p} - \kappa^{\psi} E_{k+1}^p \right), \\
I_{k+1} &= \sum_{j=0}^{k-1} I_0^{(j)} \frac{t_{k+1}^j}{j!} + \frac{h^{\psi}}{\Gamma(\psi+2)} \sum_{j=0}^{k} (q_{j,k+1}) \left(\kappa^{\psi} \sigma_e E_j - (\gamma_h^{\psi} + \gamma_n^{\psi}) I_j - \delta_i^{\psi} I_j \right) \\
&\quad + \frac{h^{\psi}}{\Gamma(\psi+2)} \sum_{j=0}^{k} (q_{k+1,k+1}) \left(\kappa^{\psi} \sigma_e E_{k+1}^p - (\gamma_h^{\psi} + \gamma_n^{\psi}) I_{k+1}^p - \delta_i^{\psi} I_{k+1}^p \right),
\end{aligned}
$$

$$
\begin{aligned}
P_{k+1} &= \sum_{j=0}^{k-1} P_0^{(j)} \frac{t_{k+1}^j}{j!} + \frac{1}{\Gamma(\psi)} \sum_{j=0}^{k} \left(q_{j,k+1}\right) \left(\kappa^\psi \sigma_s E_j - (\gamma_h^\psi + \gamma_n^\psi) P_j - \delta_p^\psi P_j\right) \\
&\quad + \frac{1}{\Gamma(\psi)} \sum_{j=0}^{k} \left(q_{k+1,k+1}\right) \left(\kappa^\psi \sigma_s E_{k+1}^p - (\gamma_h^\psi + \gamma_n^\psi) P_{k+1}^p - \delta_p^\psi P_{k+1}^p\right), \\
A_{k+1} &= \sum_{j=0}^{k-1} A_0^{(j)} \frac{t_{k+1}^j}{j!} + \frac{h^\psi}{\Gamma(\psi+2)} \sum_{j=0}^{k} \left(q_{j,k+1}\right) \left(\kappa^\psi (1 - \sigma_e - \sigma_s) E_j\right) \\
&\quad + \frac{h^\psi}{\Gamma(\psi+2)} \sum_{j=0}^{k} \left(q_{k+1,k+1}\right) \left(\kappa^\psi (1 - \sigma_e - \sigma_s) E_{k+1}^p\right), \\
H_{k+1} &= \sum_{j=0}^{k-1} H_0^{(j)} \frac{t_{k+1}^j}{j!} + \frac{h^\psi}{\Gamma(\psi+2)} \sum_{j=0}^{k} \left(q_{j,k+1}\right) \left(\gamma_h^\psi (I_j + P_j) - \gamma_p^\psi H_j - \delta_h^\psi H_j\right) \\
&\quad + \frac{h^\psi}{\Gamma(\psi+2)} \sum_{j=0}^{k} \left(q_{k+1,k+1}\right) \left(\gamma_h^\psi (I_{k+1}^p + P_{k+1}^p) - \gamma_p^\psi H_{k+1}^p - \delta_h^\psi H_{k+1}^p\right), \\
R_{k+1} &= \sum_{j=0}^{k-1} R_0^{(j)} \frac{t_{k+1}^j}{j!} + \frac{h^\psi}{\Gamma(\psi+2)} \sum_{j=0}^{k} \left(q_{j,k+1}\right) \left(\gamma_n^\psi (I_j + P_j) + \gamma_p^\psi H_j\right) \\
&\quad + \frac{h^\psi}{\Gamma(\psi+2)} \sum_{j=0}^{k} \left(q_{k+1,k+1}\right) \left(\gamma_n^\psi (I_{k+1}^p + P_{k+1}^p) + \gamma_p^\psi H_{k+1}^p\right), \\
D_{k+1} &= \sum_{j=0}^{k-1} D_0^{(j)} \frac{t_{k+1}^j}{j!} + \frac{h^\psi}{\Gamma(\psi+2)} \sum_{j=0}^{k} \left(q_{j,k+1}\right) \left(\delta_i^\psi I_j + \delta_p^\psi P_j + \delta_h^\psi H_j\right) \\
&\quad + \frac{h^\psi}{\Gamma(\psi+2)} \sum_{j=0}^{k} \left(q_{k+1,k+1}\right) \left(\delta_i^\psi I_{k+1}^p + \delta_p^\psi P_{k+1}^p + \delta_h^\psi H_{k+1}^p\right),
\end{aligned}
$$

where

$$
q_{j,k+1} = \begin{cases} k^{\psi+1} - (k-\psi)(k+1)^\psi, & \text{if } j = 0, \\ (k-j+2)^{\psi+1} + (k-j)^{\psi+1} - 2(k-j+1)^{\psi+1}, & \text{if } 1 \le j \le k, \\ 1, & \text{if } j = k+1. \end{cases} \tag{32}
$$

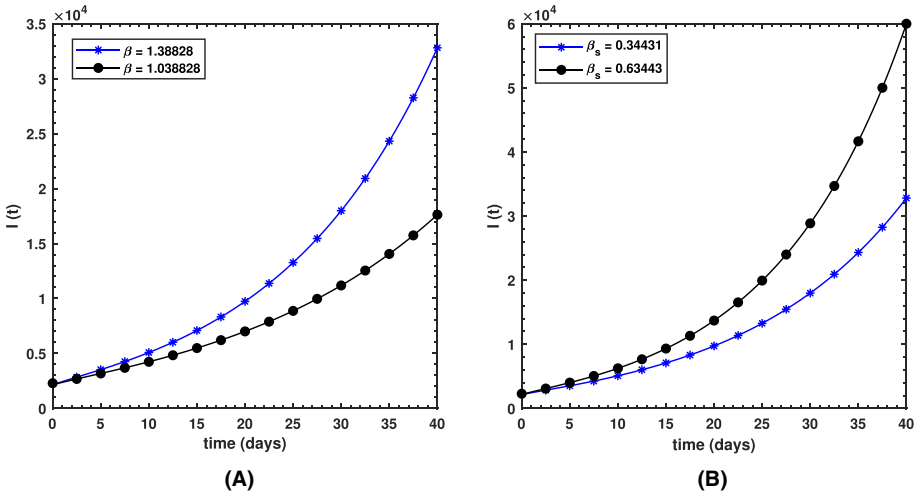

FIGURE 5 Behavior of the symptomatic and infectious class $I(t)$ for (A) decreasing values of β (transmission coefficient from infected individuals) and (B) increasing values of β_s (transmission coefficient due to super-spreaders) [Colour figure can be viewed at wileyonlinelibrary.com]

In the above numerical solver, the superscript (p) denotes the predictor part of the solver which is determined in the following way:

$$
\begin{aligned}
S^p_{k+1} &= \sum_{j=0}^{k-1} S_0^{(j)} \frac{t^j_{k+1}}{j!} + \frac{h^\psi}{\Gamma(\psi+1)} \sum_{j=0}^{k} (w_{j,k+1}) \left(-\beta^\psi \frac{I_j S_j}{N_j} - r\beta^\psi \frac{H_j S_j}{N_j} - \beta_s^\psi \frac{S_j P_j}{N_j} \right), \\
E^p_{k+1} &= \sum_{j=0}^{k-1} E_0^{(j)} \frac{t^j_{k+1}}{j!} + \frac{h^\psi}{\Gamma(\psi+1)} \sum_{j=0}^{k} (w_{j,k+1}) \left(\beta^\psi \frac{I_j S_j}{N_j} + r\beta^\psi \frac{H_j S_j}{N_j} + \beta_s^\psi \frac{S_j P_j}{N_j} - \kappa^\psi E_j \right), \\
I^p_{k+1} &= \sum_{j=0}^{k-1} I_0^{(j)} \frac{t^j_{k+1}}{j!} + \frac{h^\psi}{\Gamma(\psi+1)} \sum_{j=0}^{k} (w_{j,k+1}) \left(\kappa^\psi \sigma_e E_j - (\gamma_h^\psi + \gamma_n^\psi) I_j - \delta_i^\psi I_j \right), \\
P^p_{k+1} &= \sum_{j=0}^{k-1} P_0^{(j)} \frac{t^j_{k+1}}{j!} + \frac{h^\psi}{\Gamma(\psi+1)} \sum_{j=0}^{k} (w_{j,k+1}) \left(\kappa^\psi \sigma_s E_j - (\gamma_h^\psi + \gamma_n^\psi) P_j - \delta_p^\psi P_j \right), \\
A^p_{k+1} &= \sum_{j=0}^{k-1} A_0^{(j)} \frac{t^j_{k+1}}{j!} + \frac{h^\psi}{\Gamma(\psi+1)} \sum_{j=0}^{k} (w_{j,k+1}) \left(\kappa^\psi (1 - \sigma_e - \sigma_s) E_j \right), \\
H^p_{k+1} &= \sum_{j=0}^{k-1} H_0^{(j)} \frac{t^j_{k+1}}{j!} + \frac{h^\psi}{\Gamma(\psi+1)} \sum_{j=0}^{k} (w_{j,k+1}) \left(\gamma_h^\psi (I_j + P_j) - \gamma_p^\psi H_j - \delta_h^\psi H_j \right), \\
R^p_{k+1} &= \sum_{j=0}^{k-1} R_0^{(j)} \frac{t^j_{k+1}}{j!} + \frac{h^\psi}{\Gamma(\psi+1)} \sum_{j=0}^{k} (w_{j,k+1}) \left(\gamma_n^\psi (I_j + P_j) + \gamma_p^\psi H_j \right), \\
D^p_{k+1} &= \sum_{j=0}^{k-1} D_0^{(j)} \frac{t^j_{k+1}}{j!} + \frac{h^\psi}{\Gamma(\psi+1)} \sum_{j=0}^{k} (w_{j,k+1}) \left(\delta_i^\psi I_j + \delta_p^\psi P_j + \delta_h^\psi H_j \right),
\end{aligned}
$$

where

$$w_{j,k+1} = (k+1-j)^\psi - (k-j)^\psi.$$

Based upon the numerical solver stated above, we have simulated the proposed model to observe transmission dynamics of the symptomatic and infectious $I(t)$ in particular. This is the class we are most interested in. Having varied some biological parameters, important dynamics of the infection is revealed. As seen in (A) plot of Figure 5 that a 25% decrease in the value of β brings a substantial decrease in the behavior of infectious population whereas about 84% increase in β_s almost doubles the infectious population as observed in (B) plot of the Figure 5. Similarly, relative transmissibility of hospitalized patients play a vital role in transmission dynamics of the disease since (A) plot of the Figure 6 reveals that keeping r low is important to reduce the infections while (B) plot shows that the rate at which exposed become infectious (κ) will also slightly contribute towards increase of the disease.

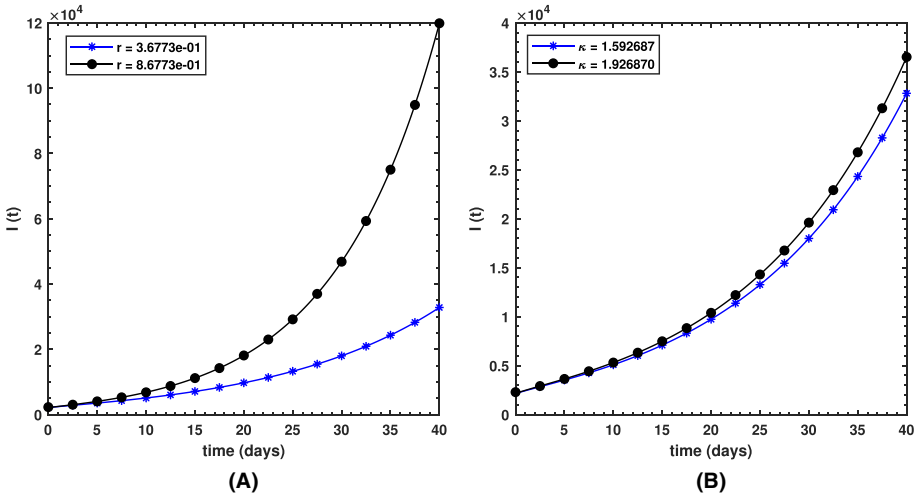

FIGURE 6 Behavior of the symptomatic and infectious class $I(t)$ for (A) increasing values of r (relative transmissibility of hospitalized individuals) and (B) increasing values of κ (rate for exposed to become infectious) [Colour figure can be viewed at wileyonlinelibrary.com]

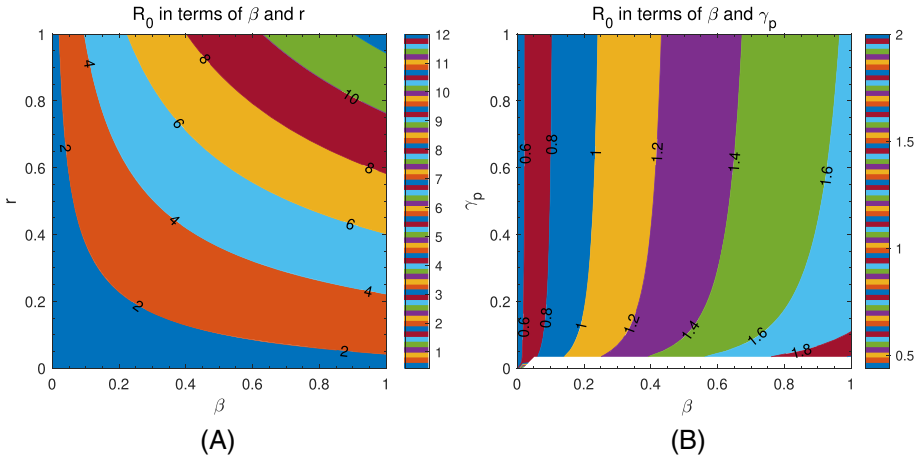

FIGURE 7 Contour plots for behavior of the basic reproduction number based upon (A) β (transmission coefficient from infected individuals) and r (relative transmissibility of hospitalized individuals); and (B) β (transmission coefficient from infected individuals) and γ_p (recovery rate of hospitalized individuals) [Colour figure can be viewed at wileyonlinelibrary.com]

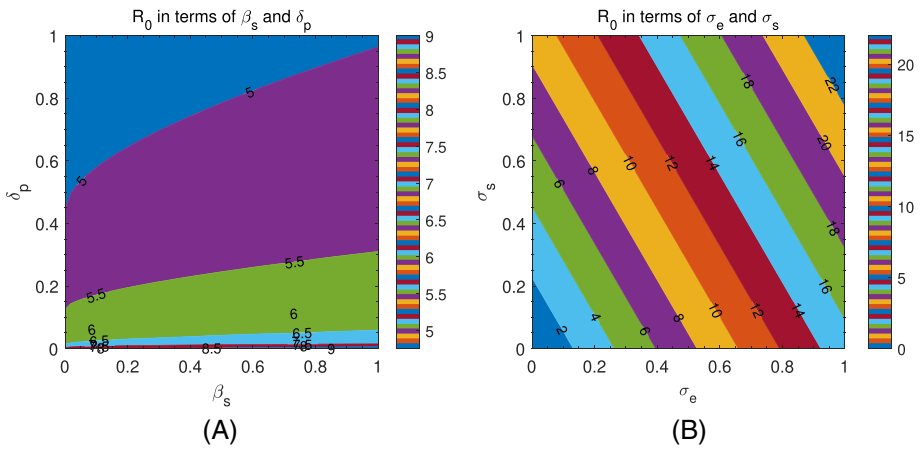

FIGURE 8 Contour plots for behavior of the basic reproduction number based upon (A) β_s (transmission coefficient due to super-spreaders) and δ_p (disease induced death rate due to super-spreaders); and (B) σ_e (rate of exposed to become infected) and σ_s (rate of exposed to become super-spreaders) [Colour figure can be viewed at wileyonlinelibrary.com]

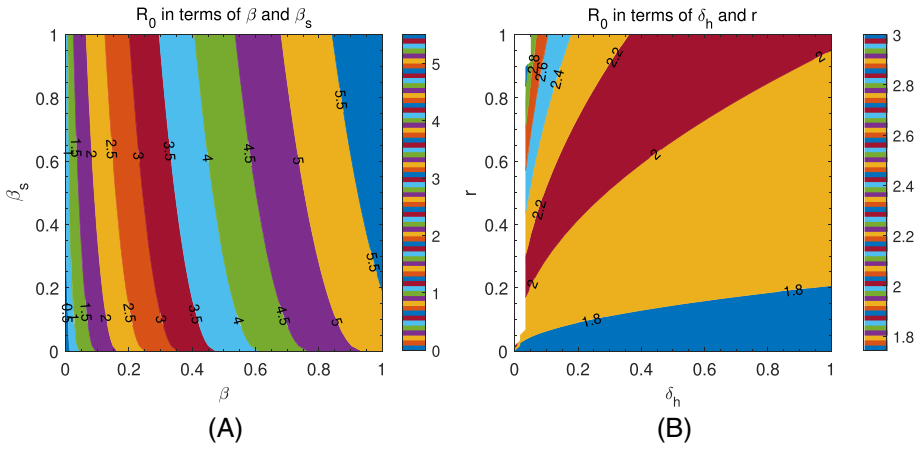

FIGURE 9 Contour plots for behavior of the basic reproduction number based upon (A) β (transmission coefficient from infected individuals) and β_s (transmission coefficient due to super-spreaders); and (B) δ_h (disease induced death rate due to hospitalization) and r (relative transmissibility of hospitalized individuals) [Colour figure can be viewed at wileyonlinelibrary.com]

For any infectious disease, it is very important for health service providers to know about the rate at which one infectious case can, on average, infect otherwise susceptible population. It is therefore important to check profile for the basic reproduction number. We have randomly chosen some parameters to see their combined effects on $\mathcal{R}_0$. As can be observed in Figure 7 that combined effects of β and r are higher than the combined effects of β and γ_p on $\mathcal{R}_0$. Figure 8 shows that the even small values of β_s and δ_p constitute together larger values of $\mathcal{R}_0$ and same is true for combined effects of σ_e and σ_s on $\mathcal{R}_0$. It is essential to keep β and β_s smaller simultaneously in order to control the spread of the disease, and this is what is revealed in (A) plot of the Figure 9 while relative transmissibility of hospitalized individuals versus (r) disease induced death rate due to hospitalization (δ_h) also contribute towards increase of $\mathcal{R}_0$ as shown by (B) plot of the Figure 9.

6 | CONCLUSIONS

This research analysis has proposed and investigated an epidemiological model of deterministic type for ongoing corona virus pandemic. The model assumes memory effects and thus designed under a fractional Caputo operator. The proposed fractional model was successfully tested with related real data originated from Pakistan, and it was made dimensionally consistent unlike models in previous literature under the Caputo operator. Moreover, existence and uniqueness conditions have been investigated and stability analysis along with iterative solution under Caputo are also proved using the concept of fixed points. The basic reproduction number $\mathcal{R}_0$ is computed to be about 6.5894 which is an alarming sign for policy makers. It has been observed in the present research study that transmissibility β, β_s, and r plays an important role for widespread of the disease. One of the novel achievements in the present research study is the computation of optimized value of fractional order ψ which ultimately produced reasonably small error of magnitude 10^{-2}. Numerical simulations prove that the social distancing, periodic lockdown and staying home are the best effective measures in order to fight with the disease. This has been concluded on the basis of profile for the basic reproduction number $\mathcal{R}_0$ wherein number of contacts of an infectious case is the major reason for the menace.

AUTHOR CONTRIBUTION

All authors have equal contributions.

CONFLICT OF INTEREST

The authors declare no potential conflict of interests.

ORCID

Nguyen Huy Tuan https://orcid.org/0000-0002-6962-1898
Dumitru Baleanu https://orcid.org/0000-0002-0286-7244

REFERENCES

1. Batista M. Estimation of the final size of the coronavirus epidemic by the SIR model. ResearchGate; 2020.
2. Victor AO. Mathematical predictions for COVID-19 as a global pandemic. medRxiv; 2020.
3. Ming WK, Huang J, Zhang CJ. Breaking down of healthcare system: mathematical modelling for controlling the novel coronavirus (2019-nCoV) outbreak in Wuhan, China. bioRxiv; 2020.
4. Nesteruk I. Statistics based predictions of coronavirus 2019-nCoV spreading in mainland China. medRxiv; 2020.
5. Ndaırou F, Area I, Nieto JJ, Torres FMT. Mathematical modeling of COVID-19 transmission dynamics with a case study of Wuhan. *Chaos, Solitons Fractals*. 2020;135:109846. https://doi.org/10.1016/j.chaos.2020.109846
6. Kim Y, Lee S, Chu C, Choe S, Hong S, Shin Y. The characteristics of Middle Eastern respiratory syndrome coronavirus transmission dynamics in South Korea. *Osong Publ Health Res Perspectives*. 2016;7:49–55. https://doi.org/10.1016/j.phrp.2016.01.001
7. Alasmawi H, Aldarmaki N, Tridane A. Modeling of a super-spreading event of the mers- corona virus during the hajj season using simulation of the existing data. *Int J Stat Med Biol Res*. 2017;1:24–30.
8. Podlubny I. *Fractional Differential Equations*. San Diego: Acad. Press; 1989.
9. Kumar D, Singh J, Tanwar K, Baleanu D. A new fractional exothermic reactions model having constant heat source in porous media with power, exponential and Mittag-Leffler laws. *Int J Heat Mass Transfer*. 2019;138:1222–1227.
10. Yang X-J, Baleanu D. Fractal heat conduction problem solved by local fractional variation iteration method. *Thermal Sci*. 2013;17(2):625–628.
11. Magin RL. Fractional calculus models of complex dynamics in biological tissues. *Comput Math Appl*. 2010;59:1586–1593.
12. Diethelm K. A fractional calculus based model for the simulation of an outbreak of dengue fever. *Nonlin Dyn*. 2013;71(4):613–619.
13. Baleanu D, Diethelm K, Scalas E, Trujillo JJ. *Fractional Calculus: Models and Numerical Methods*, Vol. 3. Boston: World Scientific; 2012.
14. Ullah S, Khan MA, Farooq M, Hammouch Z, Baleanu D. A fractional model for the dynamics of tuberculosis infection using Caputo-Fabrizio derivative. *Discrete Contin Dyn Syst*. 2020;13:975–993.
15. Wu GC, Baleanu D. Discrete fractional logistic map and its chaos. *Nonlinear Dynam*. 2014;75:283–287.
16. Qureshi S, Yusuf A, Shaikh AA, Inc M, Baleanu D. Fractional modeling of blood ethanol concentration system with real data application. *Chaos: An Interdiscipl J Nonlin Sci*. 2019;29(1):13143.
17. Qureshi S, Yusuf A. Modeling chickenpox disease with fractional derivatives: from Caputo to Atangana-Baleanu. *Chaos, Solitons Fractals*. 2019;122:111–118.
18. Kilbas AA, Srivastava HM, Trujillo JJ. *Theory and Applications of Fractional Differential Equations*. Amsterdam: Elsevier; 2006.

19. Aliyu AI, Inc M, Yusuf A, Baleanu D. A fractional model of vertical transmission and cure of vector-borne diseases pertaining to the Atangana–Baleanu fractional derivatives. *Chaos, Solitons Fractals*. 2018;116:268–277.
20. Nguyen Huy T, Baleanu D, Tran Ngoc T, O'Regan D, Can NH. Final value problem for nonlinear time fractional reaction-diffusion equation with discrete data. *J Comput Appl Math*. 2020;376:112883.
21. Arshad S, Defterli O, Baleanu D. A second order accurate approximation for fractional derivatives with singular and non-singular kernel applied to a HIV model. *Appl Math Comput*. 2020;374:125061.
22. Baleanu D, Jajarmi A, Mohammadi H, Rezapour Sh. A new study on the mathematical modelling of human liver with Caputo-Fabrizio fractional derivative. *Chaos Solitons Fractals*. 2020;134:109705.
23. Baleanu D, Diethelm K, Scalas E, Trujillo J. *Fractional Calculus Models and Numerical Methods*. 2nd ed., Series on Complexity, Nonlinearity and Chaos. Singapore: World Scientific; 2006.
24. Feng YY, Yang XJ, Liu JG. On overall behavior of Maxwell mechanical model by the combined Caputo fractional derivative. *Chin J Phys*. 2020;66:269–276.
25. Yang XJ, Feng YY, Cattani C, Inc M. Fundamental solutions of anomalous diffusion equations with the decay exponential kernel. *Math Methods Appl Sci*. 2019;42(11):4054–4060.
26. Yang XJ. *General Fractional Derivatives: Theory, Methods and Applications*. New York: CRC Press; 2019.
27. Liu JG, Yang XJ, Feng YY. On integrability of the time fractional nonlinear heat conduction equation. *J Geometry Phys*. 2019;144:190–198.
28. Liu JG, Yang XJ, Feng YY. Analytical solutions of some integral fractional differential–difference equations. *Modern Phys Lett B*. 2020;34(1):2050009.
29. Taylor AE, Lay DC. *Introduction to Functional Analysis*. New York: Wiley; 1980.
30. Wang Z, Yang D, Ma T, Sun N. Stability analysis for nonlinear fractional-order systems based on comparison principle. *Nonlinear Dyn*. 2014;75(1-2):387–402.
31. Van den Driessche P, Wanmough J. Reproduction numbers and sub-threshold endemic equilibria for compartimental models of disease transmition. *Mathem Biosci*. 2002;180:29–48.
32. Ullah S, Khan MA, Farooq M. A fractional model for the dynamics of TB virus. *Chaos, Solitons Fractals*. 2018;116:63–71.
33. Khan MA, Ullah S, Farooq M. A new fractional model for tuberculosis with relapse via Atangana–Baleanu derivative. *Chaos, Solitons Fractals*. 2018;116:227–238.
34. Diethelm K, Ford NJ, Freed AD. Detailed error analysis for a fractional Adams method. *Numer Algo*. 2004;36(1):31–52.
35. Diethelm K. An algorithm for the numerical solution of differential equations of fractional order. *Electron Trans Numer Anal*. 1997;5(1):1–6.
36. Diethelm K, Freed AD. The FracPECE subroutine for the numerical solution of differential equations of fractional order. *Forschung und Wissenschaftliches Rechnen*. 1998;1999:57–71.

How to cite this article: Tuan NH, Tri VV, Baleanu D. Analysis of the fractional corona virus pandemic via deterministic modeling. *Math Meth Appl Sci*. 2021;44:1086–1102. https://doi.org/10.1002/mma.6814